

Mid-infrared spectro-interferometric observation of the Mira variable RR Sco with the VLTI/MIDI instrument

K. Ohnaka^a, T. Driebe^a, K.-H. Hofmann^a, Th. Preibisch^a, D. Schertl^a, G. Weigelt^a,
M. Wittkowski^b

^a Max-Planck-Institut für Radioastronomie, D-53121 Bonn, Germany

Contact: kohnaka@mpifr-bonn.mpg.de

^b European Southern Observatory, D-85748 Garching, Germany

1. Introduction

Mass loss in asymptotic giant branch (AGB) stars is believed to play an important role in the chemical evolution of the Galaxy, since nuclear processed material is dredged up to the surface and finally returned to the interstellar space via mass loss. However, the mass loss mechanism in AGB stars is not yet fully understood. In order to better understand the mass loss phenomenon in Mira-type AGB stars, it is crucial to obtain a comprehensive picture of the region where mass outflows are expected to be initiated, that is, the region between the top of the photosphere and the inner edge of the expanding dust shell. Mid-infrared interferometry provides a unique opportunity to probe the circumstellar environment of Mira variables. The MIDI instrument at VLTI has a particularly great potential with its spectro-interferometric capability, which enables us to directly observe the spatial structures of molecular and dust formation regions. We present the first spectrally dispersed N -band interferometric observations of the Mira variable RR Sco with VLTI/MIDI, together with K -broadband observations using VLTI/VINCI.

2. MIDI and VINCI observations of RR Sco

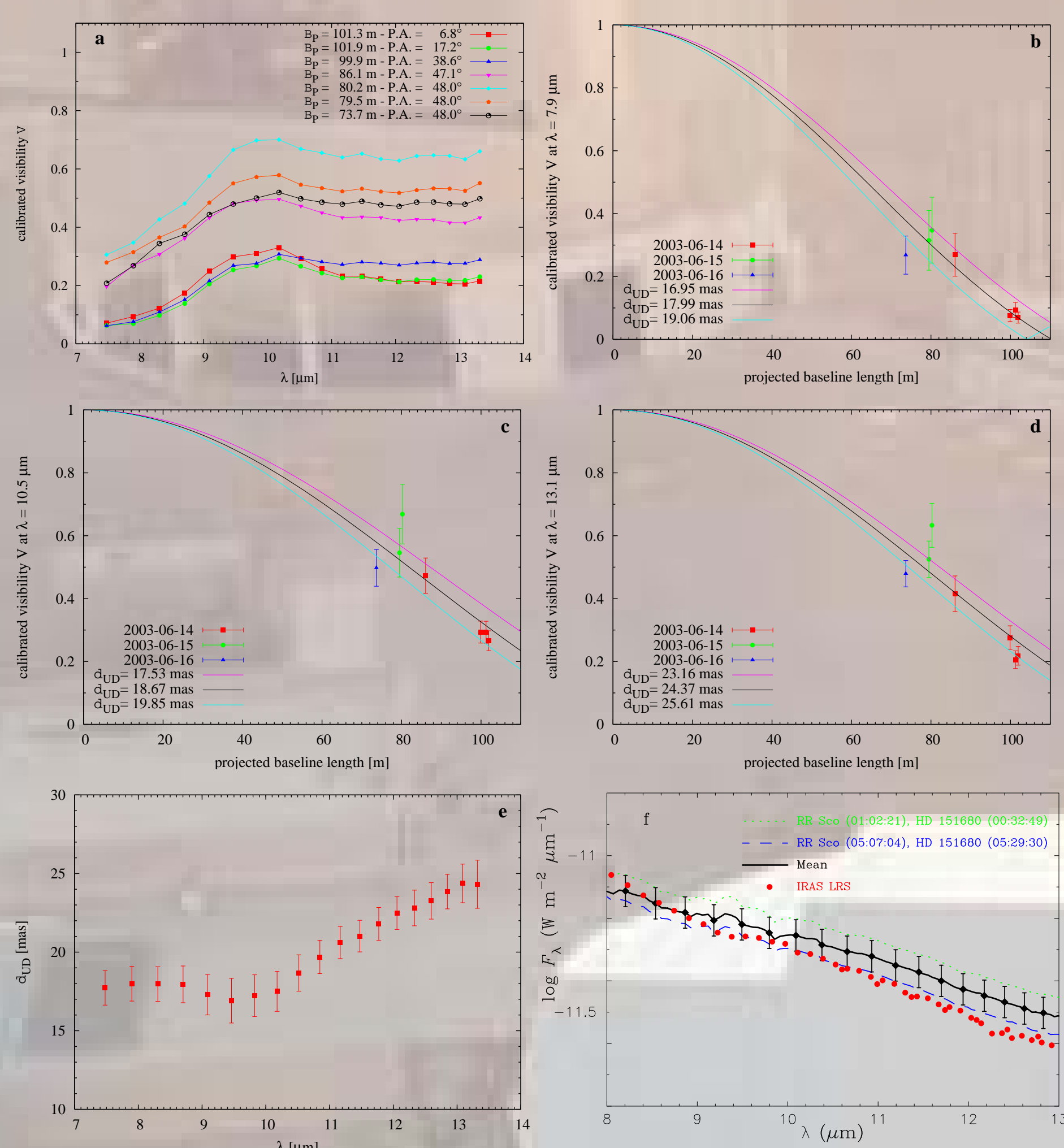


Fig. 1: **a:** Visibility as a function of wavelength for different projected baseline lengths ranging from 74 m to 102 m. For the sake of clarity, error bars are omitted in this panel. **b:** Visibility as a function of the projected baseline for $\lambda = 7.9 \mu\text{m}$. In addition, three uniform-disk fits are shown, representing the best-fitting model as well as a lower and an upper boundary fit curve. The data can be fitted with a uniform disk with a diameter of $d_{\text{UD}} = 18.0 \pm 1.1 \text{ mas}$. **c:** Same as **b**, but for $\lambda = 10.5 \mu\text{m}$. The uniform-disk fit yields $d_{\text{UD}} = 18.7 \pm 1.2 \text{ mas}$. **d:** Same as **b**, but for $\lambda = 13.1 \mu\text{m}$. The uniform-disk fit yields $d_{\text{UD}} = 24.4 \pm 1.2 \text{ mas}$. **e:** Uniform-disk diameter as a function of wavelength. The diameters are derived from uniform-disk fits using all seven averaged visibility data points of RR Sco, as exemplarily shown in **b**, **c**, and **d** for three representative wavelengths. **f:** Absolutely calibrated spectra of RR Sco. The dashed and dotted lines represent the calibrated spectra of RR Sco derived from two data sets obtained on 2003 Jun 14, using HD 151680 as a spectrophotometric standard star. The black solid line and the filled diamonds represent the mean of the above two spectra. The IRAS LRS is plotted with the filled circles.

- Mid-infrared uniform-disk diameters are constant between 8 and 10 μm and monotonically increase longward of 10 μm .

- Mid-infrared uniform-disk diameters (~ 18 –25 mas) are more than twice as large as that measured in the K band ($10.2 \pm 0.5 \text{ mas}$) using VINCI.

- Consistent with the trend found in Mira variables: the angular size increases toward longer wavelengths.

3. Modeling

We interpret the MIDI and VINCI observations in terms of dense warm molecular envelope, whose presence was revealed by ISO observations in other Mira variables (e.g., Tsuji et al. 1997, A&A, 320, L1; Yamamura et al. 1999, A&A, 348, L55; Cami et al. 2000, A&A, 360, 562; Matsuura et al. 2002, A&A, 383, 972), and an optically thin dust shell. The schematic view of our model is depicted in Fig. 2.

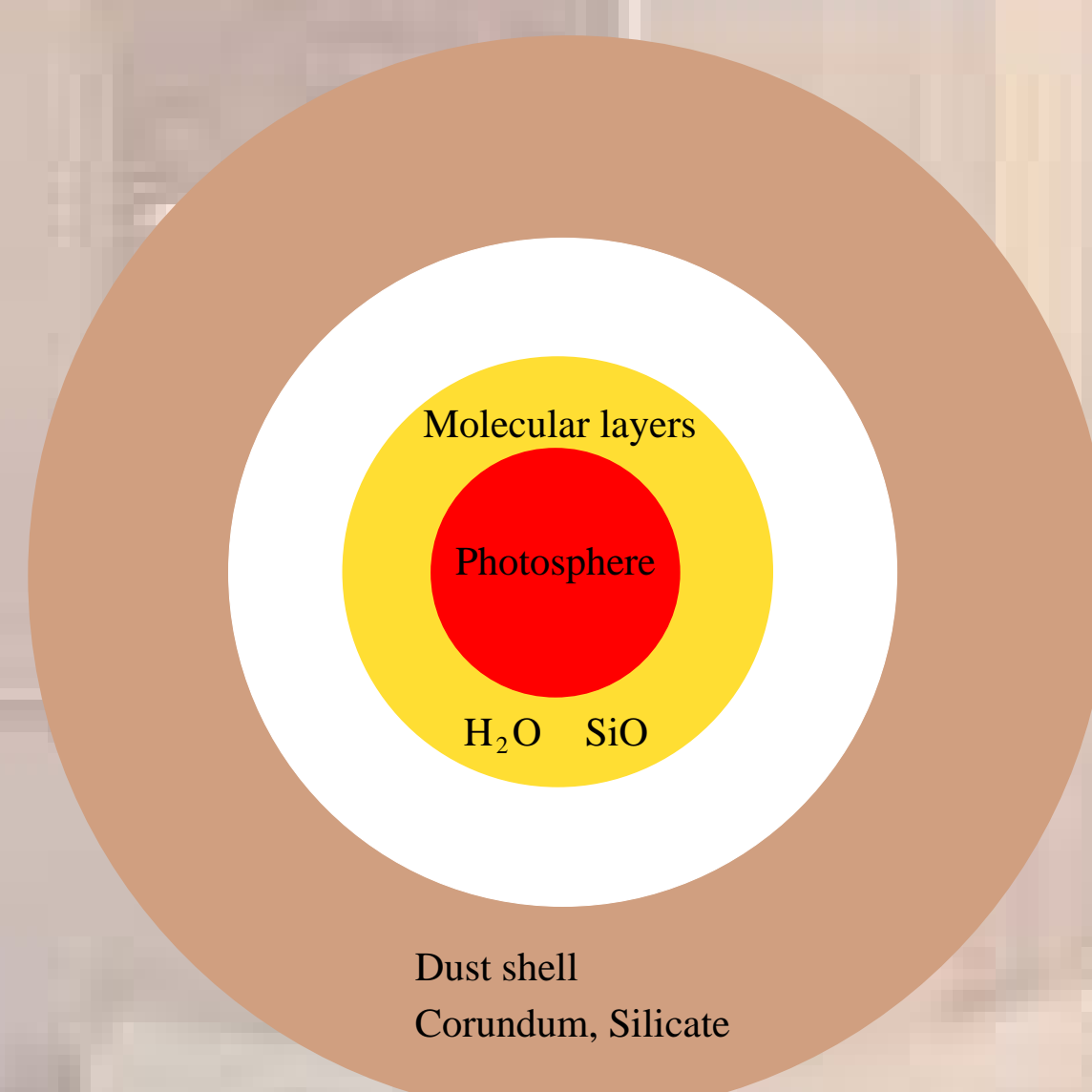


Fig. 2: Schematic view of our model. The central star is surrounded by the warm molecular envelope consisting of H_2O and SiO , which is represented by a layer with a constant temperature and density. An optically thin dust shell consisting of silicate and corundum is also added.

The monochromatic intensity profiles and the spectra are calculated with H_2O lines (mainly pure-rotation transitions) taken from the HITEMP database and the fundamental bands of SiO . Details of our modeling is described in Ohnaka et al. (2005, A&A, 429, 1057).

4. Results

The results of our modeling are shown in Figs. 3 and 4. Both figures show the visibilities, uniform-disk diameters, and the spectrum predicted by the best-fit model. In Fig. 3, the results are convolved to a spectral resolution of 10000 to better show the presence of H_2O and SiO line emission. In Fig. 4, the results are convolved to a spectral resolution of 30, which is used in the MIDI observations.

- The uniform-disk diameters between 8 and 10 μm , which are twice as large as the K -band diameter, can be explained by the optically thick emission from the $\text{H}_2\text{O}+\text{SiO}$ layer.

- The parameters of the molecular layer: radius = $2.3 R_\star$, temperature = 1400 K, H_2O and SiO column densities = $3 \times 10^{21} \text{ cm}^{-2}$, $1 \times 10^{20} \text{ cm}^{-2}$, respectively.

- The increase of the uniform-disk diameter longward of 10 μm can be explained by the contribution of the optically thin dust shell. The parameters of the dust shell: inner radius = 7 – $8 R_\star$ (temperature = $\sim 700 \text{ K}$), optical depth at 10 μm = ~ 0.025 . Silicate: $\sim 20\%$, Corundum: $\sim 80\%$.

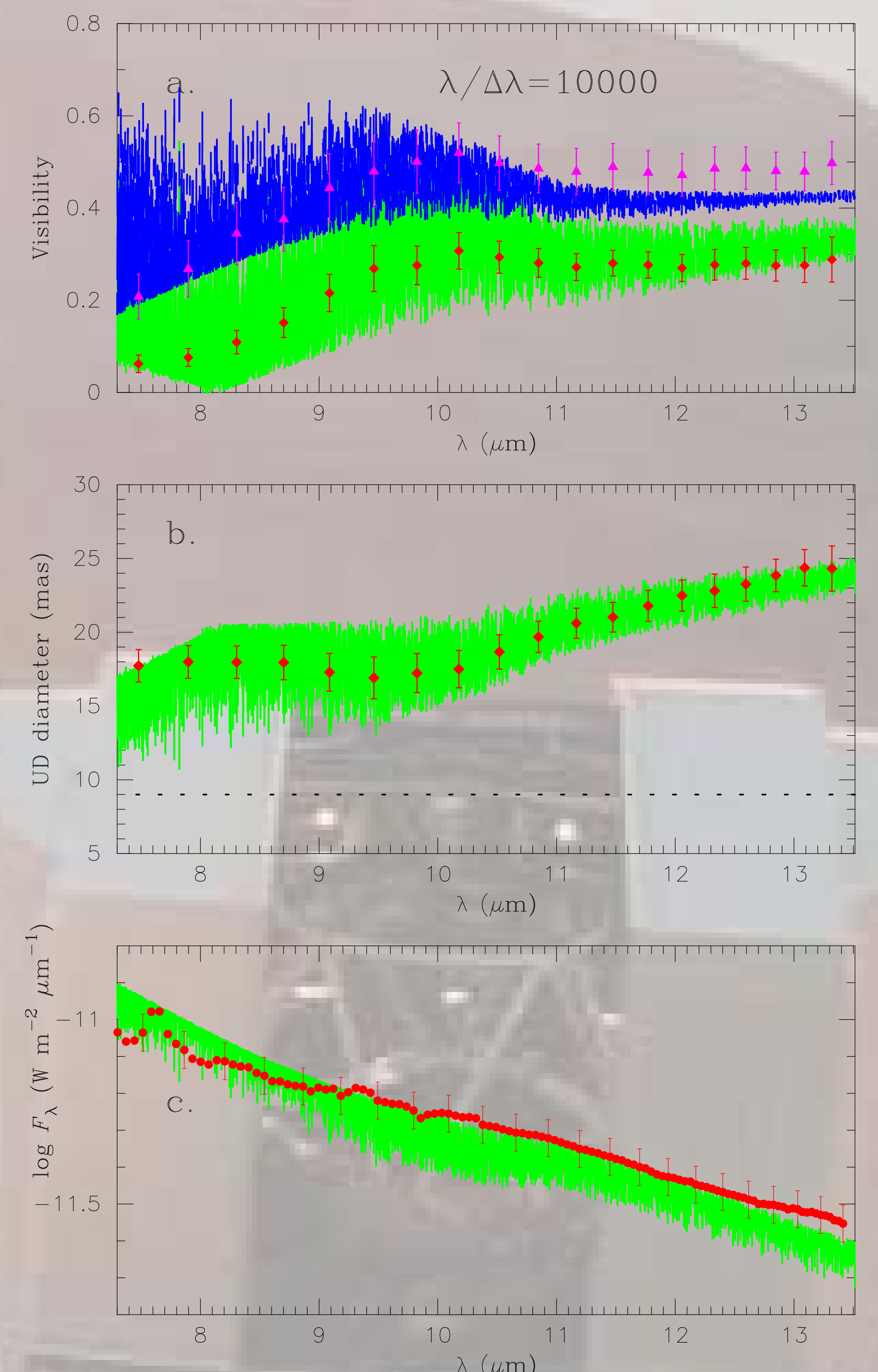


Fig. 3: Comparison between the observed visibility (**a**), uniform-disk diameter (**b**), and spectrum (**c**) and those predicted by the best-fit model for RR Sco. The results are convolved with a spectral resolution of 10000. **a:** Visibilities observed with the 99.9 m baseline (diamonds) and 73.7 m (triangles). The corresponding predicted visibilities are represented with the green and blue lines, respectively. **b:** Filled diamonds: observed values. Green line: best-fit model. The dotted line represents the continuum angular diameter assumed in the calculation. **c:** Filled circles: observed spectrum of RR Sco. Green line: best-fit model.

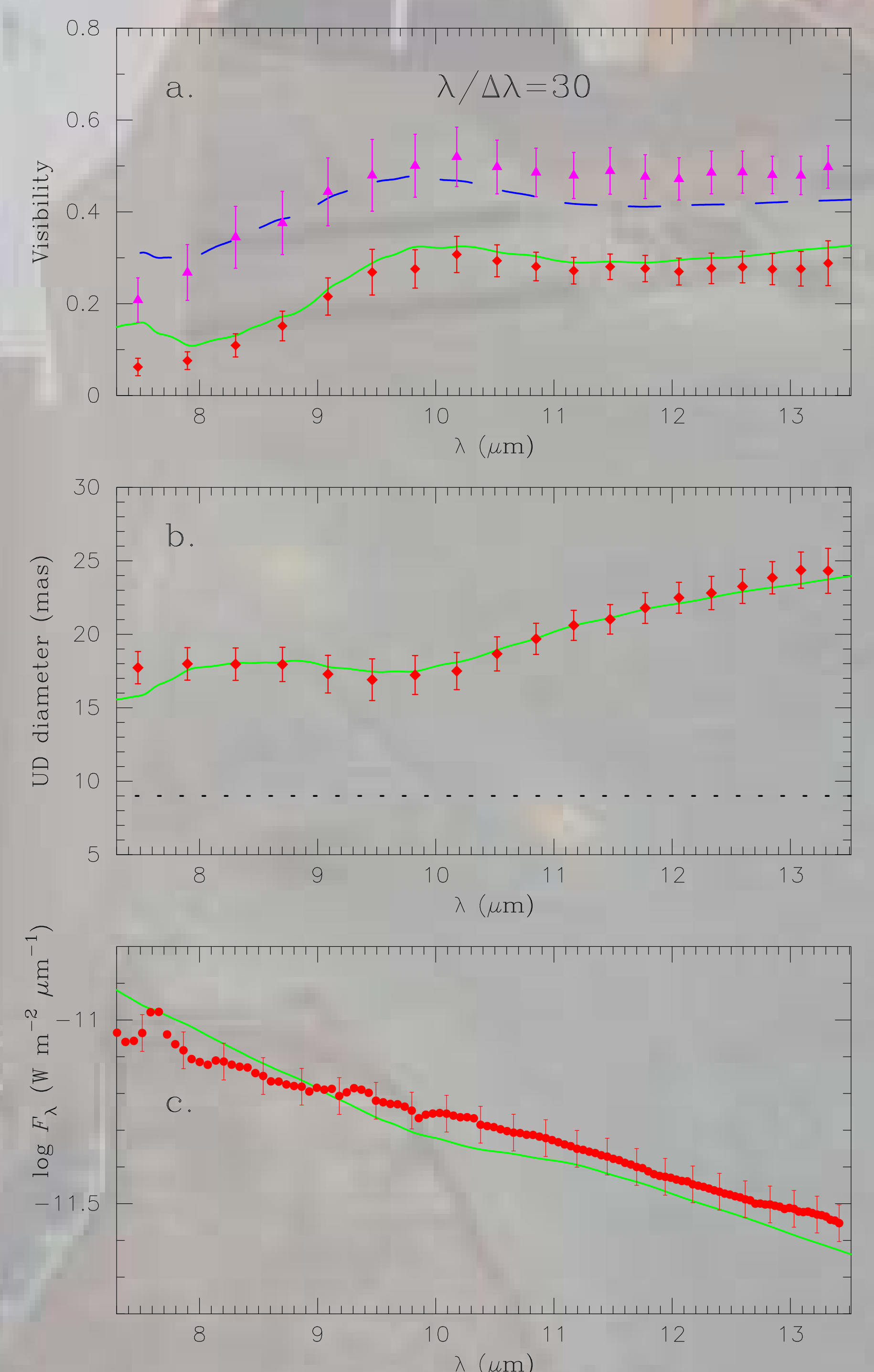


Fig. 4: Same as Fig. 3, but convolved with a spectral resolution of 30, which is used in the MIDI observations.